ERJ Express. **Published on April 22, 2010 as doi: 10.1183/09031936.00097609**

FIZZ1 potentiates the carbachol-induced tracheal smooth muscle contraction

Hang Chen, Bruce A Jacobson, Lawrence Mason, Stanley F Wolf and Michael R Bowman

Inflammation/Immunology, Pfizer Research, 200 Cambridge Park Drive, Cambridge MA 02140

Key words: Airway epithelium, MLCK, MLC20, c-Raf, ERK1/2, MAPK

Running title: Effect of FIZZ1 on mouse tracheal rings

Address reprint requests to Michael R Bowman PhD

Inflammation/Immunology

Pfizer Research

200 Cambridge Park Drive

Cambridge MA 02140

Phone: 617-665-5403

FAX: 617-665-5584

E-mail address: MRBowman@wyeth.com

ABSTRACT

FIZZ1 is an adipokine highly expressed under inflammatory conditions, and yet, little is known of its function. In this study we examine the expression and function of FIZZ1 in an ovalbumin mouse model of asthma.

Trachea from either naïve or ovalbumin-sensitized and challenged mice were compared for transcriptional, functional and proteomic differences using gene microarrays, ex vivo tracheal contraction, immunohistochemistry and Western blot analysis.

FIZZ1 was expressed in ovalbumin-treated, but not naïve, trachea. Naïve trachea incubated with recombinant FIZZ1 exhibited denuded epithelium and contractile hyper-responsiveness. The FIZZ1-incubated trachea also exhibited an associated increased expression of phospho-c-Raf, phosphor-ERK1/2, phospho-p38, MLCK and MLC-20.

These data demonstrate that FIZZ1 regulates TSM contraction through impairment of the epithelium and activation of the MAPK pathway in muscle.

INTRODUCTION

FIZZ1, Resistin-like molecule-α, is a secreted protein of the resistin family of adipokines. It is released from a variety of cell types including airway epithelial cells. FIZZ1 was first identified in a murine model of experimental asthma and an increase in its mRNA and protein levels were seen in a variety of Th2-mediated inflammatory settings [1], suggesting a role in the pathogenesis of Th2-mediated diseases. FIZZ1 protein administered into the lungs of mice has been shown to induce macrophage infiltration into the BAL and collagen deposition in the lung [2, 3]. Additional studies revealed that FIZZ1 protein has vasoconstrictive properties and is antiapoptotic for lung fibroblasts [4, 5]. Though a biological effect of FIZZ1 has not been elucidated on intact TSM, the strong induction of expression and these reports of pleiotropic biological activities led us to hypothesize that FIZZ1 may influence the functional behavior of TSM. This could provide important clues to FIZZ1's role in such pulmonary diseases as asthma and thus may provide novel therapeutic opportunities [6-8].

In this study, increased levels of FIZZ1 mRNA and protein were demonstrated in trachea and/or BAL from the ovalbumin(OA) model. Impairment of the epithelial layer was observed in rFIZZ1-treated trachea with an associated increased contractile response, over-expression of MLCK, MLC-20 and activation of signaling molecules linked to MAPK pathway.

MATERIALS AND METHODS

Preparation of animals and trachea

Specific pathogen-free male BALB/C mice (5 wks) were housed at Pfizer Research under pathogen-free conditions for the duration of the experiments. All studies were conducted in accordance with the National Institutes of Health Guide for the Care and Use of Laboratory Animals as well as following guidelines from, and with the approval of, the Institutional Animal Care and Use Committee of Pfizer Research.

Animals were grouped as phosphate buffered saline (PBS)-sensitized and -challenged (PBS/PBS), OA-sensitized and PBS-challenged (OA/PBS), and OA-sensitized and -challenged mice (OA/OA). Mice were injected intraperitoneally with PBS or OA (20μg) with 2.25mg $Al(OH)_3$ on day 0 and 14. From day 25 to 34, mice were challenged with PBS or OA (5%) for 30 min per day for 10 consecutive days.

Tracheal rings from naïve mice were isolated and cultured overnight in DMEM in the absence and presence of 10 or 100nM rFIZZ1 (Leinco Technologies, USA) as well as 0.1 ng/ml lipopolysaccharide (100nM rFIZZ1 contains an endotoxin level < 0.1ng). In a separate study, the tension in fresh trachea and BAL cell counts were measured at 24 hours after the last treatment of mice receiving an intranasal PBS, 0.1ng/ml LPS or 100nM rFIZZ1 (once a day x 5 days).

Cell counts and protein preparation

BAL from each sacrificed mouse was centrifuged (1200 rpm x 5 min). The total BAL cells were counted and a sample applied to a glass slide, stained with Hema 3 Stain Set (Fisher Scientific, USA), for the differential count of cells.

TSM tissue was collected by cutting away cartilage and physically scraping off the epithelium under a light microscope. The PBS- and rFIZZ1-treated trachea and TSM were homogenized in lysis buffer (mM) containing 20 MOSP, 2.0 EGTA, 5.0 EDTA, 30 sodium fluoride, 40 β-glycerophosphate, 20 sodium orthovanadate, 1.0 phenylmethylsulfonyl-fluoride, 3.0 benzamidine, 0.005 pepstatin A, 0.01 leupeptin and 0.5% Triton X-100 at pH 7.2. The supernatants were cleared by centrifugation and the protein concentrations measured by BCA Assay.

Examination of airway epithelium and epithelial cell culture and assay

The status of the epithelial layer was examined in whole/sectional trachea with and without 100nM rFIZZ1 or mechanically removing the intraluminal surface by gently rubbing with polyethylene tubing (PE10) connected to a needle (30G1/2) followed by perfusion with 1.0 ml of air bubbles and then 1.0 ml Krebs-Henseleit (K-H) solution (9). The trachea stained with H & E was photographed using computer-based imaging under a light microscope.

Mouse tracheal epithelial cell (MTEC) culture was performed as previously described, with minor modification [10, 11]. Briefly, trachea was incubated in 1.5 mg/ml pronase for 18 h at 4°C. Cells were treated with 0.5 mg/ml crude pancreatic DNase I (Sigma-Aldrich) on ice for 5 min. After incubation in tissue culture plates for 3-4 h in 5% CO_2 at 37°C, nonadherent cells were incubated in a plate coated with type I rat tail collagen (BD Biosciences) in modified BEBM (Lonza, MD USA) containing 10μg/ml insulin, 5 μg/ml transferrin, 25 ng/ml epidermal growth factor, 5 μg/ml epinephrine and 30 μg/ml bovine pituitary extract, 0.5nM Hydrocortisone, 25ng/ml hEGF, 15nM Triiodothyronine, 0.25μg/ml Gentamicin/amphotericin-B and 0.01 μM retinoic acid in 5% CO_2 at 37°C. MTEC were seeded on polycarbonate semipermeable membrane (0.4 μM pore size, Corning, NY) and media was removed from upper chamber to establish an air-liquid interface, lower chambers only were provided with BEBM/DMEM (1:1, v/v) containing 7.5μl retinoic acid and 750μl BSA in presence and absence of LPS and rFIZZ1.

Apoptotic MTEC death was examined in MTEC cultures (5 x 10^4/ml) treated with PBS, 0.1ng/ml LPS or 100nM rFIZZ1 using Cell Death Detection ELISA^{plus} (Roche) and calculated as an index of a fold change over a control.

Nitric oxide (NO) was examined by measuring an end product, [nitrite]. Briefly, aliquots (50 μl) of supernatants from treated MTEC were mixed with 50 μl Griess reagent (Bio-Rad, Hercules, CA) at room temperature for 10 min. The absorbance was read at 540nm in an automated microplate reader [12].

Pharmacodynamic studies

The isometric tensions of TSM were examined, as previously described [13]. Briefly, a change in the tension was recorded with a MP15 system (BIOPAC Systems, Inc., Goleta, CA). A [CCh]-response curve was completed in tracheal rings in absence and presence of either rFIZZ1 or LPS. Concentration of the agonist was increased only after the force responses to the previous

concentration had stabilized. In addition, a heat-inactivated rFIZZ1 (70^0C x 60 min) was examined to verify its biological activity.

Electrophoresis and quantification of proteins

Aliquots of tracheal (100μg/well) and TSM (10μg/well) lysates were size-fractionated on a 4-20% SDS-PAGE gel and transferred to a nitrocellulose membrane and blocked with 5% nonfat dried milk in TBS. The membrane was individually incubated with primary antibodies to FIZZ1 (Antigenix America Inc., Huntington Station, NY), MLCK, MLC-20, α-actin, Giα1,2, Gqα11, β-actin (Sigma-Aldrich, St Louis, MO), Gα12/13 (Santa Cruz Biotechnology, Inc., Santa Cruz, CA), c-Raf, phospho-c-Raf, ERK1/2, phospho-ERK1/2, p38 MAPK and phospho-p38 MAPK (Cell Signaling, Inc., Danvers, MA) at 4^0C overnight and then incubated with HPR-conjugated secondary antibodies. Proteins were quantified using ImageJ and relative band intensity calculated as % of the intensity of the β-actin protein band.

GeneChips

Total RNA of trachea from treated mice was extracted and RNA was purified with Qiagen RNeasy minicolumns. This RNA was linearly amplified and biotin-labeled with Nugen's Ovation System (NuGEN Technologies, Inc., San Carlos, CA) [14]. Approximately 1.5 μg of purified and fragmented biotinylated cRNA, together with Wyeth standards for quantifying the amount of each transcript, was hybridized to the mouse gene chip array for 16-18 hours. GeneChips were scanned with an Agilent GeneArray scanner. The signals were normalized and quantified using Gene Logic's MAS 5.0 software.

Data analysis

At the end of experiment, trachea were blotted on a gauze pad and weighed. Results were calculated as tension/TSM weight (mg/mg) and expressed as a percentage (%) of the mean value of the maximal responses in PBS-treated trachea.

All values were expressed as Mean ± SEM. Comparisons within groups of contractile agonist were performed by one-way analysis of variance (ANOVA). Student's unpaired t-test was used to compare the effects of PBS, LPS and rFIZZ1. A p value of less than 0.05 was considered significant.

RESULTS

Features of OA model

The CCh-induced contraction was increased in trachea from the OA/OA-treated mice (Fig 1A). The difference in the force level was statistically significant when comparing either PBS/PBS or OA/PBS vs OA/OA ($P < 0.05$, $n = 6$). The cellular composition of the BAL was determined for the treated mice (Fig 1B-D). A large increase in the number of total BAL cells, lymphocytes and eosinophils was observed in the OA/OA-treated mice as compared to those from the other two groups. ($P < 0.01$, $n = 6$). The level of FIZZ1 mRNA expression in tracheal tissue was examined by transcriptional profiling and shown in Fig 2. The fold change in FIZZ1 mRNA expression in trachea from OA/OA-treated mice was increased 33-fold over that from either PBS/PBS- or OA/PBS-treated mice. In contrast to the inability to measure FIZZ1 protein from either PBS/PBS- or OA/PBS-treated mice, the FIZZ1 protein was easily detected in the BAL and trachea from the OA/OA-treated mice (Fig 2). These data, together with those from previous publications, indicate that FIZZ1 is induced in Th2 inflammatory situations.

Histological examination of airway epithelium

There were no tissue edema, unusual epithelial denudation and/or patchy shedding of epithelial cells on the luminal side of the PBS/PBS-treated fresh trachea or the PBS-treated cultured trachea (Fig 3). In contrast, there was an obvious infiltration of inflammatory cells into epithelial layer/tracheal wall in OA/OA-exposed trachea (A). In association with this infiltration, epithelial cells were destroyed with epithelial denudation or patchy shedding of the epithelial cells in the trachea. In rFIZZ1-treated cultured trachea, the epithelial layer was thinner and some of epithelium was denuded (B). However, the epithelial layer in fresh trachea from rFIZZ1-exposed mice was intact with no epithelial denudation and inflammatory cells infiltrate in the trachea (C). With the mechanical removal of epithelium, histological observation showed a similar state of epithelial denudation to that seen in rFIZZ1-treated trachea.

Effect of rFIZZ1, heat-inactivated FIZZ1 and LPS on trachea

rFIZZ1-treated trachea induced a significantly increased force response (Fig 4A) as compared to PBS-treated trachea ($P < 0.05$, $n = 6$). The increased expression of MLCK and MLC-20 was likewise detected in rFIZZ1-treated TSM (Fig 4A, Lower). Heat-treated rFIZZ1 and

LPS had no effect on the CCh-mediated force response (Fig 4B, Lower). There was a statistically significant difference detected in the force response between the native rFIZZ1-treated group and the other groups ($P < 0.05$, $n = 6$).

Force response of fresh trachea and BAL cell counts

The BAL cell counts and tensions of fresh trachea were examined 24 hours after the last treatment of mice receiving intranasal doses of PBS, LPS or rFIZZ1 (Fig 5). Significant increases in the CCh-evoked force response (A) measured in the fresh trachea and in the number of BAL cells (B) were detected in rFIZZ1-challenged mice compared to either PBS- or LPS-exposed mice ($P < 0.05$, $N = 5$). In addition, a slight increase in the cell counts was observed in LPS-treated vs PBS-treated mice ($P < 0.05$).

rFIZZ1 effects on MTEC and epithelium-denuded trachea

In order to explore the mechanisms responsible for the FIZZ1-mediated loss of tracheal epithelium, MTEC apoptosis was investigated. A significant increase ($P < 0.05$ or 0.01; $N = 3$) in MTEC apoptosis was detected at all of the time points after rFIZZ1 treatment compared to LPS treatment (Fig 6A). However, no induction of nitrite production was measured at any time point (Fig 6B). With mechanical removal of the epithelium, there were significant differences in the force response between trachea with and without epithelium as well as untreated and rFIZZ1-treated trachea without epithelium ($P < 0.05$, $n = 8$-19) (Fig 6C). Together these data indicate that FIZZ1 cause epithelial cell death and this cell death together with a direct effect on the smooth muscle induces an increased tracheal contractile response.

Protein expression in rFIZZ1-treated trachea

Upon initiation of receptor-mediated signaling, the activation state of second messenger proteins is altered. We investigated the state of several G protein-couple receptors as well as members of the c-Raf/MAPK/Erk pathways. The expression levels of α-actin, Giα1,2, Gqα11, and Gα12/13 were similar between PBS- and rFIZZ1-treated trachea (Fig7 A). The expression of phosphorylated and unphosphorylated c-Raf, ERK1/2 and p38 MAPK showed a similar level of expression for most of the unphosphorylated proteins, whereas phospho-c-Raf, -ERK1/2, and -p38 MAPK in trachea and TSM tissues all statistically increased in expression after rFIZZ1 treatment ($P < 0.01$ or 0.05 vs PBS, $n = 3$) (Fig7 B-D). These data indicate that

correlated with an increase in TSM contraction, FIZZ1 induces an activation of the c-Raf/MAPK signaling pathway.

DISCUSSION

Several studies have tested the hypothesis that nonspecific AHR in asthma is caused by increased force generation in the smooth muscle due to either increases in the size and number of individual muscle cells or a modification of the muscle's intracellular contractile signaling pathways [15-17]. In initial experiments, a mouse AHR model with a 10-day OA challenge was initially performed following a previously reported protocol modeling abnormal TSM function (18, 19). Our results show that this model is associated with a significant increase in CCh-evoked force and a large inflammatory infiltrate, comprised mainly of lymphocytes and eosinophils, into the BAL. In association with these findings, transcriptional profiling revealed that FIZZ1 mRNA expression in the trachea from OA/OA-treated mice was up-regulated 30-fold over that from either PBS/PBS- or OA/PBS-treated animals. These data identified FIZZ1 as an inducible gene product within a process of local allergen-triggered airway inflammation. In support of this finding, FIZZ1 protein was detected in the BAL and trachea from OA/OA-treated mice, suggesting the particular importance of FIZZ1 as a proinflammatory mediator propagating allergic inflammation. It has been previously reported that FIZZ1 protein expression was significantly increased in the BAL from OA-treated mice, reaching levels as high as 5μg/ml [1]. Due to the correlation of increased FIZZ1 protein expression and the induction of AHR in inflamed trachea, we postulated that FIZZ1 contributes to a cascade of effects culminating in TSM dysfunction.

Since FIZZ1 is found in airway epithelium [1, 4], it suggests that this protein exerts its effects in the local environment. We found in a direct rFIZZ1-treated ring the epithelial layer was significantly thinner and lacked histological intactness with epithelial denudation. This reveals that FIZZ1 acts on the airway epithelium and leads to a direct loss of the epithelial barrier similar to that seen in OA/OA-exposed trachea where an infiltration is associated with patchy epithelial layer destruction. Since epithelial damage is clinically associated with human asthma (20, 21) and often caused by a release of major basic proteins from infiltrating inflammatory cells into the inflamed airways [22, 23], our data suggest that the in vitro epithelial damage observed in the FIZZ1-exposed trachea is consistent with that of the in vivo asthmatic airway.

FIZZ1 was found to directly induce an increase in the CCh-generated force in TSM.

In support of this result, expression levels of MLCK and its primary substrate, MLC-20, were significantly increased in the TSM. This finding provides an important molecular basis to fully understand the force development observed in the FIZZ1-treated trachea and supports the conclusion that FIZZ1 alters the contractile property of the TSM by influencing the expression level of contractile proteins within the tissue. It is well documented that a key event in the regulation of TSM contraction is the phosphorylation/dephosphorylation of the regulatory light chain of myosin catalyzed by the calmodulin-activated MLCK [24-26]. An exposure to inflammatory mediators induces smooth muscle dysfunction with an increase in MLCK/MLC-20 expression [27], suggesting that the TSM contractile apparatus may be surrounded and bombarded by inflammatory mediators. Due to the histological finding that culturing with FIZZ1 resulted in epithelial denudation, there was a concern that the increased force response was a consequence of the epithelial damage. Because there is no known intrinsic linkage in the contractile mechanism between epithelial damage and the activation of MLCK, the FIZZ1 effect on CCh-elicited contraction should be considered a dual entity of two separate effects, one on the epithelium and another on the TSM. In support of the observed effect of FIZZ1 protein on cultured trachea, mice given an in vivo administration of rFIZZ1 protein showed significant increases in both the force response of freshly isolated trachea and in the number of BAL cells compared to either PBS- or LPS-treated animals. Because the epithelial layer of freshly isolated trachea from FIZZ1-treated mice was intact with no cellular infiltrate, it leads us to conclude that FIZZ1 protein participates in modulating lung inflammation and the increased force activity in the trachea is due to a dysfunction of TSM rather than an influx of inflammatory cells.

Due to the histological changes in epithelial layer observed in rFIZZ1-treated trachea, the apoptosis of MTEC was determined within the time period of the study. The results show a significant increase in apoptosis, indicating that FIZZ1 acts directly on airway tissue enhancing epithelial cell death. Further investigation showed no change in [nitrite] throughout this time period, suggesting a loss of NO was not responsible for the increased force response. In order to clarify whether or not the epithelial damage contributes to the increased force response in FIZZ1-exposed trachea, epithelial cells were mechanically removed from trachea of naïve mice. Our results show an increased force response in the epithelium-denuded trachea,

demonstrating the importance of the epithelial barrier in the protection of TSM from direct exposure to contractile agonists. Since the epithelium-denuded trachea treated with rFIZZ1 showed an increased force level as compared to that of denuded trachea without rFIZZ1 treatment, it is reasonable to conclude that this protein exerts separable effects involving both the epithelium and TSM, representing different stages in the process of abnormal smooth muscle force development.

There has been growing awareness that proinflammatory proteins are able to modulate the functional properties of TSM (13). To investigate the molecular mechanism(s) responsible for the FIZZ1-induced changes in the TSM functional response, the expression level of smooth muscle α-actin was assessed in FIZZ-1-treated trachea based on a previous report that the transfection of a FIZZ1-expressing plasmid into lung fibroblasts stimulated α-actin production and induced vasoconstrictive properties [3, 4]. Our result showed that α-actin was expressed at a similar level in both rFIZZ1- and PBS-treated tissues, indicating that FIZZ1 did not exert its effects by changing the expression of this contractile element. Since the muscarinic receptor preferentially couples to G-proteins leading to an increase in MLC-20 phosphorylation and the associated muscle contraction, it is possible that the FIZZ1 effect is mediated through the activation of Gsα, Giα, Gqα or Gα12/13, amplifying the receptor-mediated generation of second messengers [28]. Our results show that the expression of the G-proteins in rFIZZ1-treated trachea was identical to the level detected in PBS-treated trachea, indicating that changes in the expression of these G-proteins is not involved in the event.

Upon binding their cognate ligand, receptor tyrosine kinases (RTK) in the plasma membrane activate Ca^{2+} mobilization, inducing TSM force generation, through a pathway distinct from that used by the G-protein-coupled receptors [29, 30]. The activation of RTKs may produce a downstream effect contributing to the activation of c-Raf-mediated MAPK signal transduction pathways eventually leading to an increase in MLC-20 phosphorylation [31-33]. A recent study suggested that ERK1/2 and p38MAPK in fibroblasts were activated by FIZZ1 and an inhibitor of the MAPK pathway suppressed this activation [5]. Our results show that FIZZ1 treatment induces high levels of phospho-c-Raf, phospho-ERK1/2, and phospho-p38 MAPK not only in tracheal rings but also in TSM tissue, indicating that FIZZ1 is sufficient to cause the

activation of this arm of the MAPK signaling pathway and it directly acts on the TSM tissue. The lack of change in the expression levels of G proteins and the increased c-Raf/MAPK and MLC-20 phosphorylation, leads us to conclude that FIZZ1 regulation of the CCh-evoked force appears to act through a c-Raf-linked MAPK signaling cascade leading to an increase in MLC-20 phosphorylation and enhanced TSM contraction.

In conclusion, our results indicate that FIZZ1 enhances the TSM contractile response with an associated increase in MLCK and MLC-20 expression levels. The increased force generation observed in FIZZ1-treated trachea is caused by an impairment of the airway epithelium and an activation of a c-Raf-ERK1/2-p38 MAPK signaling pathway in the contracting TSM.

REFERENCES

1. Holcomb IN, Kabakoff RC, Chan B, Baker TW, Gurney A, Henzel W, Nelson C, Lowman HB, Wright BD, Skelton NJ, Frantz GD, Tumas DB, Peale FV, Shelton DL, Hebert CC. FIZZ1, a Novel Cysteine-Rich Secreted Protein Associated with Pulmonary Inflammation, Defines a New Gene Family. The EMBO Journal 2000; 19: 4046-4055.
2. Liu T, Jin H, Ullenbruch M, Hu B, Hashimoto N, Moore B, McKenzie A, Lukacs NW, Phan SH. Regulation of Found in Inflammatory Zone 1 Expression in Bleomycin-Induced Lung Fibrosis: Role of IL-4/IL-13 and Mediation via STAT-6. J Immunol 2004; 173: 3425 -3431.
3. Liu T, Dhanasekaran SM, Jin H, Hu B, Tomlins SA, Chinnaiyan AM, Phan SH. FIZZ1 Stimulation of Myofibroblast Differentiation. Am J Pathol 2004; 164: 1315-1326.
4. Teng X, Li D, Champion HC, Johns RA. FIZZ1/RELMα, a Novel Hypoxia-Induced Mitogenic Factor in Lung With Vasoconstrictive and Angiogenic Properties. Circ Res 2003; 92: 1065-1067.
5. Chung MJ, Liu T, Ullenbruch M, Phan SH. Antiapoptotic Effect of Found in Inflammatory Zone (FIZZ)1 on Mouse Lung Fibroblasts. J Pathol 2007; 212: 180-187.
6. Oliver BG, Black JL. Airway Smooth Muscle and Asthma. Allergology International 2006; 55: 215-223.
7. Halayko AJ, Tran1 T, Ji SY, Yamasaki1 A, Gosens R. Airway Smooth Muscle Phenotype and Function: Interactions with Current Asthma Therapies. Current Drug Targets 2006; 7: 525-540.
8. Solway J, Irvin CG. Airway Smooth Muscle as a Target for Asthma Therapy. N Engl J Med 2007; 356: 1367-1369.
9. Liu JQ, Yang D, Folz RJ. A novel bronchial ring bioassay for the evaluation of small airway smooth muscle function in mice. Am J Physiol Lung Cell Mol Physiol 2006; 291:L281-L288.
10. You Y, Richer EJ, Huang T, Brody SL. Growth and differentiation of mouse tracheal epithelial cells: selection of a proliferative population. Am J Physiol Lung Cell Mol Physiol 2002; 283: L1315-L1321.

11. Mathew B, Park GY, Cao H, Azim AC, Wang X, Van Breemen RB, Sadikot RT, Christman JW. Inhibitory kB kinase 2 Activates Airway Epithelial Cells to Stimulate Bone Marrow Macrophages. Am J Respir Cell Mol Biol Physiol 2007; 36: 562-572.
12. Chen H, MacLeod C, Deng B, Mason L, Kasaian M, Goldman S, Wolf S, Williams C, Bowman MR. CAT-2 Amplifies the Agonist-Evoked Force of Airway Smooth Muscle By Enhancing Spermine-Mediated Phosphatidylinositol-(4)-Phosphate-5-Kinase-γ Activity. Am J Physiol Lung Cell Mol Physiol 2007; 293: L883-L891.
13. Chen H, Tliba O, Besien CV, Panettieri RA Jr, Amrani Y. Airway Hyper-responsiveness: From Molecules to Bedside Selected Contribution: TNF-α modulates Murine Tracheal Rings Responsiveness to G-Protein-Coupled Receptor Agonists and KCl. J Appl Physiol 2003; 95: 864-872.
14. Kurn N, Chen P, Heath DJ, Kopf-Sill A, Stephens KM, Wang S. Novel Isothermal, Linear Nucleic Acid Amplification Systems for Highly Multiplexed Applications. Clinical Chemistry 2005; 51: 1973-1981.
15. Wiggs BR, Moreno R, Hogg JC, Hilliam C, Pare PD. A Model of the Mechanics of Airway Narrowing. J Appl Physiol 1990; 69: 849-60.
16. Chiba Y, Sakai H, Misawa M. Augmented Acetylcholine-Induced Translocation of RhoA in Bronchial Smooth Muscle from Antigen-Induced Airway Hyperresponsive Rats. Br J Pharmacol 2001; 133: 886-890.
17. Martin JG, Duguet A, Eidelman DH. The contribution of airway smooth muscle to airway narrowing and airway hyperresponsiveness in disease. Eur Respir J 2000; 16: 349-354.
18. Matsubara S, Li G, Takeda K, Loader JE, Pine P, Masuda ES, Miyahara N, Miyahara, S, Lucas JJ, Dakhama A, Gelfand EW. Inhibition of Spleen Tyrosine Kinase Prevents Mast Cell Activation and Airway Hyperresponsiveness. Am J Respir Crit Care Med 2006; 173: 56-63.
19. Taube C, Wei X, Swasey CH, Joetham A, Zarini S, Lively T, Takeda K, Loader J, Miyahara N, Kodama T, Shultz LD, Donaldson DD, Hamelmann EH, Dakhama A, Gelfand EW. Mast Cells, FcRI, and IL-13 Are Required for Development of Airway Hyperresponsiveness after Aerosolized Allergen Exposure in the Absence of

Adjuvant. J
Immunol 2004; 172: 6398-6406.

20. Cokugras H, Akcakaya N, Seckin I, Camcioglu Y, Sarimurat N, Aksoy F. Ultrastructural examination of bronchial biopsy specimens from children with moderate asthma. Thorax 2001; 56: 25-29
21. White SR, Dorscheid DR. Corticosteroid-Induced Apoptosis of Airway Epithelium A Potential Mechanism for Chronic Airway Epithelial Damage in Asthma. CHEST 2002; 122: 2785-2845.
22. Flavahan NA, Slifman NR, Gleich GJ, Vanhoutte PM. Human eosinophil basic protein causes hyperreactivity of respiratory smooth muscle. Am Rev Respire Dis 1988; 138: 685-688.
23. Gundel RH, Letts LG, Gleich GJ. Human eosinophil major basic protein induces airway contraction and airway hyperresponsiveness in primates. J Clin Invest 1991; 87: 1470-1473.
24. Somlyo AP, Somlyo AV. Signal Transduction and Regulation in Smooth Muscle. Nature 1994; 372: 231-236.
25. Kamm KE and Stull JT. Dedicated Myosin Light Chain Kinases with Diverse Cellular Functions. J Biol Chem 2001; 276: 4527-4530.
26. Jiang H, Rao K, Halayko AJ, Liu X, and Stephens NL. Ragweed sensitization-induced increase of myosin light chain kinase content in canine airway smooth muscle. Am J Respir Cell Mol Biol 1992; 7: 567-573.
27. Fernandes DJ, Mitchell RW, Lakser O, Dowell M, Stewart AG, and Solway J. Invited Review: Do inflammatory mediators influence the contribution of airway smooth muscle contraction to airway hyperresponsiveness in asthma? J Appl Physiol 2003; 95: 844-853.
28. Schramm CM, Grunstein MM. Assessment of Signal Transduction Mechanisms Regulating Airway Smooth Muscle Contractility. Am J Physiol Lung Cell Mol Physiol 1992; 262: L119-L139.
29. Hubbard SR, Miller WT. Receptor Tyrosine Kinases: Mechanisms of Activation and Signaling. Current Opinion in Cell Biology 2007; 19: 117-123.

30. Berlin AA, Hogaboam CM, Lukacs NW. Inhibition of SCF Attenuates Peribronchial Remodeling in Chronic Cockroach Allergen-Induced Asthma. Laboratory Investigation 2006; 86: 557-565.
31. McKay MM, Morrison DK. Integrating Signals from RTKs to ERK/MAPK. Oncogene 2007; 26: 3113-3121.
32. Klingenberg D, Gündüz D, Härtel F, Bindewald K, Schäfer M, Piper HM, Noll T. MEK/MAPK as a Signaling Element in ATP Control of Endothelial Myosin Light Chain. Am J Physiol Cell Physiol 2004; 286: C807-C812.
33. Klemke RL, Cai S, Giannini AL, Gallagher PJ, Lanerolle PD, Cheresh DA. Regulation of Cell Motility by Mitogen-activated Protein Kinase. J Cell Biol 1997; 137: 481-492.

FIGURE LEGENDS

Figure 1. Tracheal smooth muscle contractility and the number of bronchial alveolar lavage (BAL) cells are enhanced in the ovalbumin (OA) model.

Tracheal smooth muscle contractility (A) and counts of total cells, lymphocytes and eosinophils from the BAL (B - D) were examined in phosphate buffered saline (PBS)/PBS-, OA/PBS- and OA/OA-treated mice. *: $P < 0.05$ or **: $P < 0.01$ OA/OA- vs either PBS/PBS- or OA/PBS-treated mice.

Figure 2. Signal of FIZZ1 mRNA and protein expression are increased in the ovalbumin (OA) model.

The FIZZ1 mRNA expression in trachea was assayed by transcriptional profiling. FIZZ1 levels are represented as the fold change (Fc) of mRNA from trachea from mice treated with phosphate buffered saline (PBS)/PBS, ovalbumin (OA)/PBS and OA/OA vs trachea from naïve animals. The level of FIZZ1 protein in the bronchial alveolar lavage (BAL) and trachea from the treated mice was determined in reference to the level of β-actin in the tracheal sample (insert).

Figure 3. rFIZZ1 or mechanical removal results in the loss of the luminal epithelial layer.

Histological examination of airway structure and the status of the airway epithelial layer were performed on frozen tracheas (either whole or sectional) from the OA model (A) cultured trachea (B) and fresh trachea (C) treated with PBS, LPS and 100nM rFIZZ1 or tracheal rings with the epithelial cells mechanically removed (B). All sections were viewed by light microscopy at magnifications of x4.0 and x20.

Figure 4. rFIZZ1 increases carbachol (CCh)-generated TSM force.

The CCh-generated force in phosphate buffered saline (PBS)-, lipopolysaccharide (LPS)- and rFIZZ1-treated trachea was recorded as original tracings (upper panel). Cumulative concentration-response curves of isometric tension to CCh stimulation were completed in PBS- and native rFIZZ1-treated (10nM or 100nM) trachea. Myosin light chain kinase (MLCK) and myosin light chain-20 (MLC-20) protein expression levels in TSM were measured in

relation to the expression level of β-actin in the same tissue (A insert). The CCh-dose response curves were also performed in trachea treated with 0.1ng/ml of LPS, 100nM native rFIZZ1 and 100nM heat-inactivated rFIZZ1 (B). *: $P < 0.05$ rFIZZ1 vs PBS- or the heat-treated rFIZZ1 groups.

Figure 5. In vivo administration of rFIZZ1 enhances contractile response of fresh trachea and increases the BAL cell count.

Force response in freshly isolated trachea (A) and counts of BAL cells (B) were examined in mice receiving an intranasal phosphate buffered saline (PBS), 0.1ng/ml lipopolysaccharide (LPS) or 100nM rFIZZ1 (once a day for 5 days). *, **: $P < 0.05$ vs either PBS- or LPS-treated mice.

Figure 6. The effect of rFIZZ1 on mouse tracheal epithelial cell culture (MTEC) and trachea without intact epithelium.

MTEC apoptosis index (A) and [Nitrite] (B) were examined in supernatants from treated MTEC. Cumulative dose-response curves of isometric tension to CCh stimulation (C) were measured in trachea with epithelium, EP(+) and those with mechanically removed epithelium, EP(-), treated with PBS or FIZZ1. All of tension measurements for the groups (N = 8-19) are expressed as Mean ± SEM. *: $P < 0.05$, **: $P < 0.01$ and #: $P < 0.07$.

Figure 7. Phosphorylation of c-Raf/ERK1/2/p38 MAPK is increased in rFIZZ1-treated trachea.

The expression levels of α-actin and various G proteins (A), as well as proteins involved in the MAPK pathway such as c-Raf, phospho-c-Raf, ERK1/2, phospho-ERK1/2, p38 MAPK and phospho-p38 MAPK (B) were examined in either 100nM rFIZZ1- or phosphate buffered saline (PBS)-treated trachea or TSM. Quantitation of the intensity of the protein bands was performed using ImageJ (C, D). *, **, $P< 0.05$ or 0.01 vs PBS ($n = 3$).

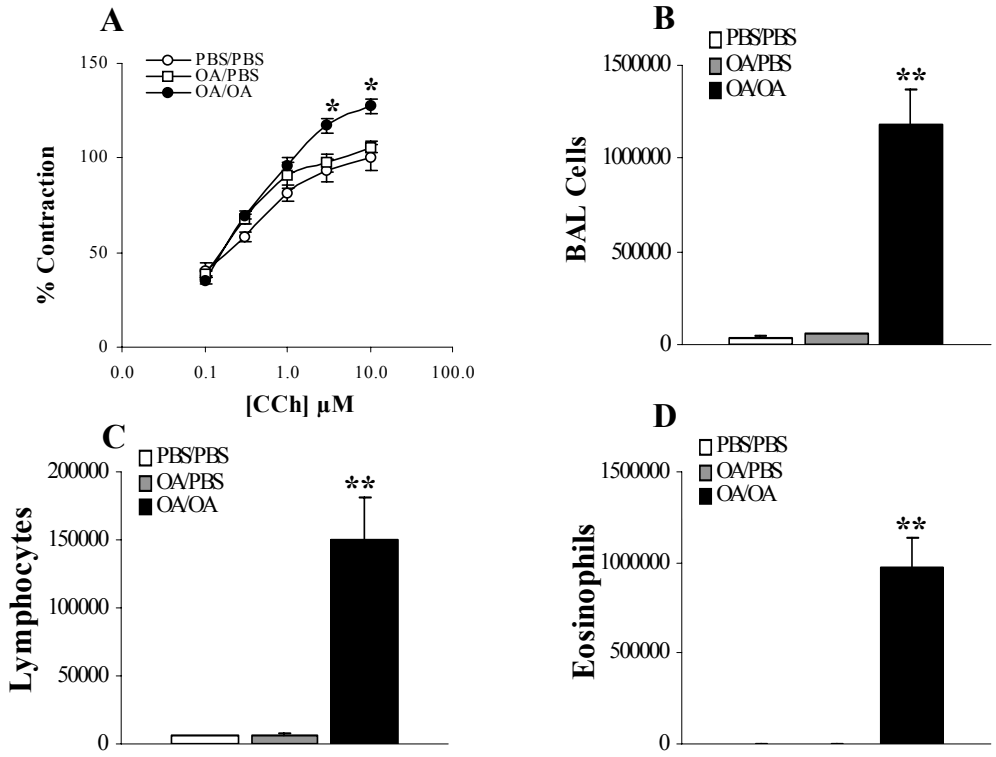
A
PBS/PBS
OA/PBS
OA/OA
% Contraction
[CCh] µM
B
BAL Cells
C
Lymphocytes
D
Eosinophils
**
*

Fig 1

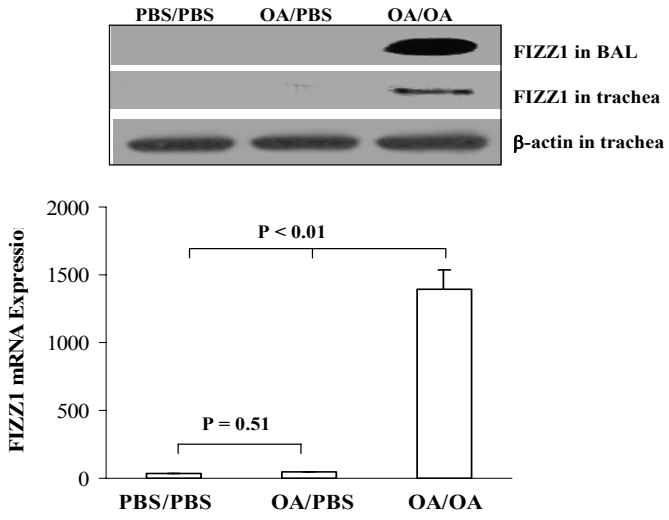
PBS/PBS
OA/PBS
OA/OA
FIZZ1 in BAL
FIZZ1 in trachea
β-actin in trachea
FIZZ1 mRNA Expressio
P < 0.01
P = 0.51

Fig 2

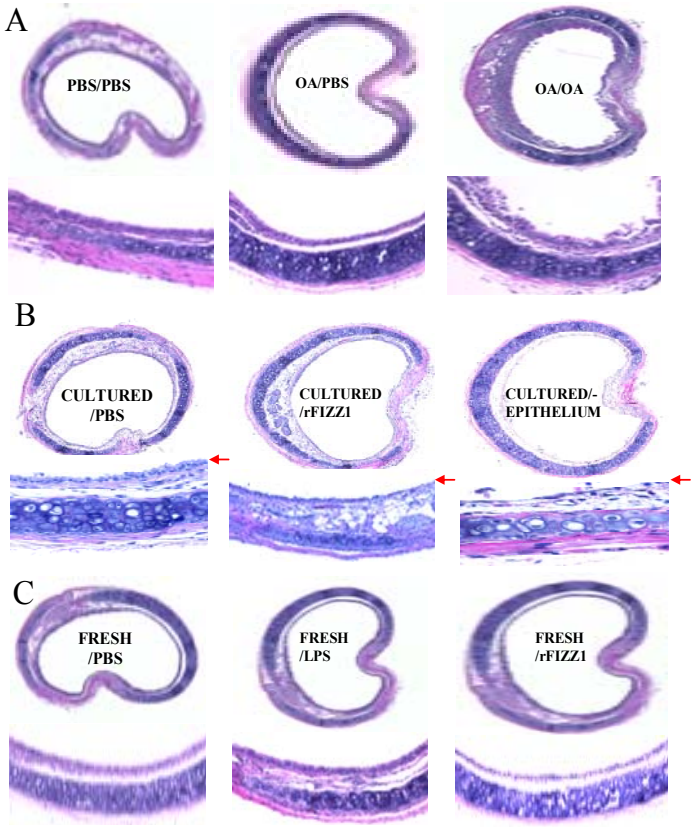
A
PBS/PBS
OA/PBS
OA/OA
B
CULTURED /PBS
CULTURED /rFIZZ1
CULTURED/- EPITHELIUM
C
FRESH /PBS
FRESH /LPS
FRESH /rFIZZ1

Fig 3

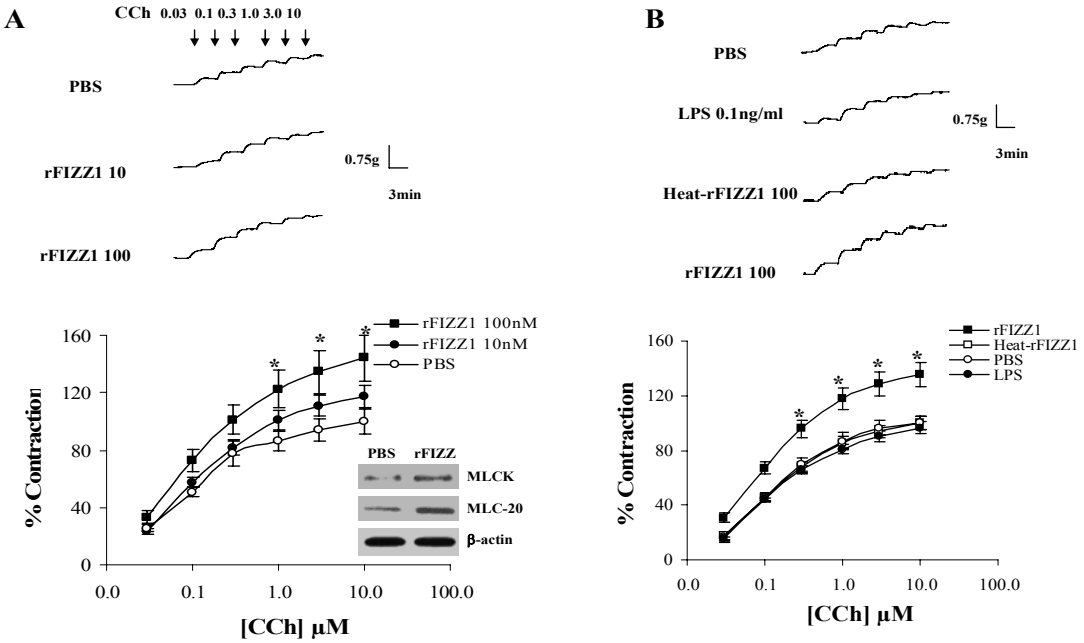
A
CCh 0.03 0.1 0.3 1.0 3.0 10
PBS
rFIZZ1 10
rFIZZ1 100
0.75g
3min
rFIZZ1 100nM
rFIZZ1 10nM
PBS
% Contraction
[CCh] μM
PBS rFIZZ
MLCK
MLC-20
β-actin
B
PBS
LPS 0.1ng/ml
Heat-rFIZZ1 100
rFIZZ1 100
0.75g
3min
rFIZZ1
Heat-rFIZZ1
PBS
LPS
% Contraction
[CCh] μM

Fig 4

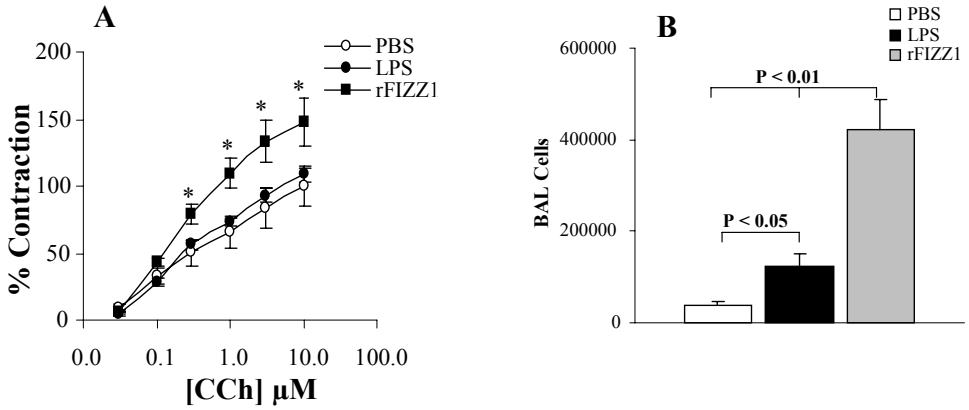
A
PBS
LPS
rFIZZ1
% Contraction
200
150
100
50
0
0.0
0.1
1.0
10.0
100.0
[CCh] µM
B
PBS
LPS
rFIZZ1
BAL Cells
600000
400000
200000
0
P < 0.01
P < 0.05

Fig 5

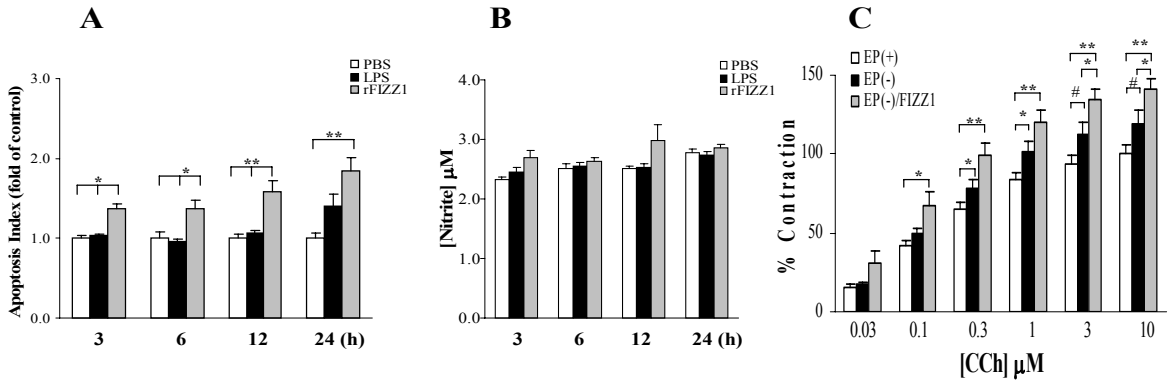
A
PBS
LPS
rFIZZ1
Apoptosis Index (fold of control)
3.0
2.0
1.0
0.0
3
6
12
24 (h)
B
PBS
LPS
rFIZZ1
[Nitrite] µM
4.0
3.0
2.0
1.0
0.0
3
6
12
24 (h)
C
EP(+)
EP(-)
EP(-)/FIZZ1
% Contraction
150
100
50
0
0.03
0.1
0.3
1
3
10
[CCh] µM

Fig 6

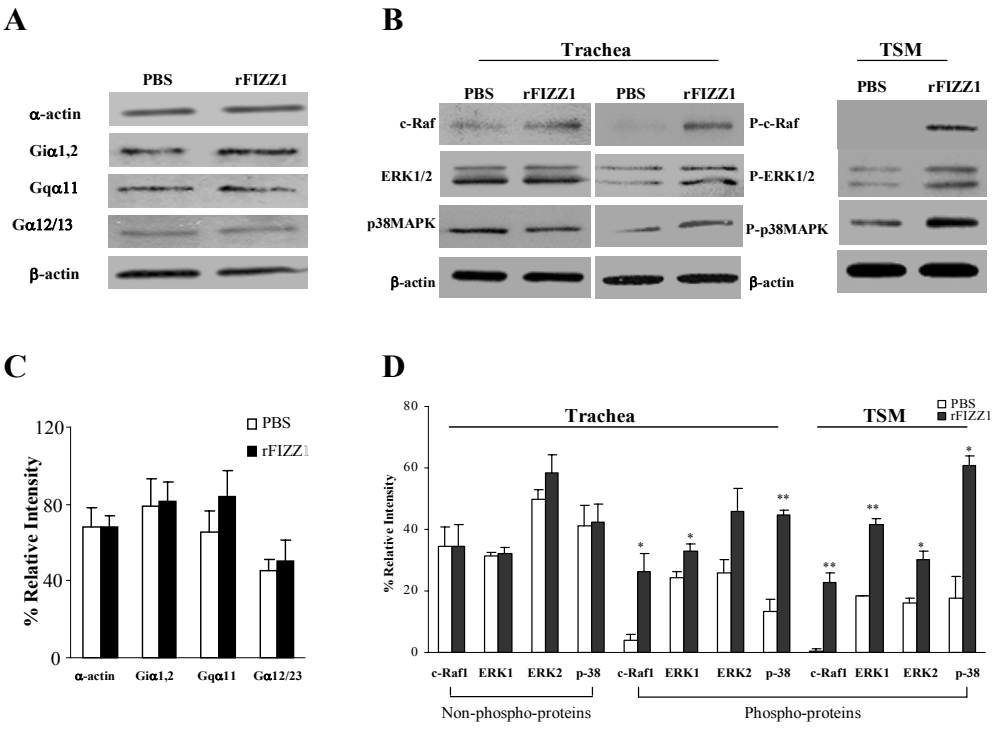
A
PBS
rFIZZ1
α-actin
Giα1,2
Gqα11
Gα12/13
β-actin
B
Trachea
TSM
PBS
rFIZZ1
PBS
rFIZZ1
PBS
rFIZZ1
c-Raf
P-c-Raf
ERK1/2
P-ERK1/2
p38MAPK
P-p38MAPK
β-actin
β-actin
C
PBS
rFIZZ1
% Relative Intensity
120
80
40
0
α-actin
Giα1,2
Gqα11
Gα12/23
D
Trachea
TSM
PBS
rFIZZ1
% Relative Intensity
80
60
40
20
0
c-Raf1
ERK1
ERK2
p-38
c-Raf1
ERK1
ERK2
p-38
c-Raf1
ERK1
ERK2
p-38
Non-phospho-proteins
Phospho-proteins

Fig 7